OPEN ACCESS
IOP Publishing
Journal of Optics
J. Opt. **16** (2014) 015301 (7pp)
doi:10.1088/2040-8978/16/1/015301

Investigating the micro-rheology of the vitreous humor using an optically trapped local probe

Fiona Watts[1], Lay Ean Tan[2,5], Clive G Wilson[2], John M Girkin[3], Manlio Tassieri[4] and Amanda J Wright[1,6]

[1] Institute of Photonics, SUPA, University of Strathclyde, Glasgow, G4 0NW, UK
[2] Strathclyde Institute for Pharmacy and Biological Sciences, University of Strathclyde, Glasgow, G4 0NR, UK
[3] Biophysical Sciences Institute, Department of Physics, University of Durham, Durham, DH1 3LE, UK
[4] Division of Biomedical Engineering, School of Engineering, University of Glasgow, Glasgow, G12 8LT, UK
[5] Ferring Controlled Therapeutics Limited, 1 Redwood Place, Peel Park Campus, East Kilbride G74 5PB, UK
[6] IBIOS, University of Nottingham, University Park, Nottingham, NG7 2RD, UK

E-mail: manlio.tassieri@glasgow.ac.uk and amanda.wright@nottingham.ac.uk

Received 20 September 2013, revised 15 November 2013
Accepted for publication 18 November 2013
Published 11 December 2013

Abstract
We demonstrate that an optically trapped silica bead can be used as a local probe to measure the micro-rheology of the vitreous humor. The Brownian motion of the bead was observed using a fast camera and the micro-rheology determined by analysis of the time-dependent mean-square displacement of the bead. We observed regions of the vitreous that showed different degrees of viscoelasticity, along with the homogeneous and inhomogeneous nature of different regions. The motivation behind this study is to understand the vitreous structure, in particular changes due to aging, allowing more confident prediction of pharmaceutical drug behavior and delivery within the vitreous humor.

Keywords: optical trapping, micro-rheology, vitreous humor
PACS numbers: 87.80Cc, 83.85Ei, 83.50.-a

(Some figures may appear in colour only in the online journal)

1. Introduction

The adult human vitreous humor occupies a volume of approximately 4 ml in the posterior segment of the eye in the space between the lens and the retina. The vitreous is composed of two phases: the bulk gel phase comprising of approximately 80% of the volume, surrounded by a liquid phase [1–3]. The major component is water (99%) with a 1% solid component, which includes collagen and the proteoglycans-chondroitin sulfate, opticin and hyaluronan [1–4]. Collagen, the principle protein constituent, is stabilized by the proteoglycans, which trap water molecules to produce a transparent hydrogel network. This physical microstructure underpins the complex viscoelastic behavior of the vitreous humor [1, 5]. Since the degree of viscosity and elasticity are modulated by the relative amount of hyaluronan and collagen, respectively [6], non-uniform distribution of these major components leads to variations in the viscoelastic properties across the vitreous humor [6–9]. Jongebloed and Worst have characterized the highly structured fibrillar networks surrounding a system of 'hollow' spaces, also

known as 'cisterns', using combinations of ink particles. The individual collagen fibers vary in density, texture and length, contributing to a three-dimensional fiber network of varying mesh diameter [10].

The inhomogeneous nature of the vitreous humor becomes more apparent with age, when the collagen fibers are aggregated and liquid pockets (lacunae) are formed within the gel phase [11, 12]. Such non-uniformity in an aging eye will have consequences in terms of drug distribution [13, 14], since the drug in the more liquid parts of the vitreous will follow convective flow processes more easily leading to increased retinal exposure [15]. In order to construct models predicting the flow patterns in the eye, a micro-rheological method is needed to quantify the local viscoelasticity.

Optical trapping is a technique whereby micron-sized particles can be trapped and manipulated in three dimensions using a laser beam and a high numerical aperture microscope objective lens [16–18]. The coherent light typically exerts a force ranging from hundreds of femtoNewtons to tens of picoNewtons on the trapped particle and can be used to calibrate interaction forces found in biology [19]. Over the last decade, there has been considerable interest in using optical tweezers to provide localized probes with which to observe the micro-rheology of the medium, which surrounds the trapped bead [19–27]. Using a fast camera or quadrant photodiode it is possible to observe the thermal Brownian motion of the optically trapped bead over time. The viscoelastic properties of the material surrounding the bead can be determined by analyzing the different frequency components of this motion. Compared to traditional rheometers, optical tweezers are able to provide the material's linear rheological properties with a spatial resolution of microns and require only a relatively small sample volume ($\sim$10 μl). Optical tweezers, therefore, provide the ideal tool to probe, map and quantify the local viscoelasticity of the vitreous humor.

Micro-rheology techniques are mainly concerned with the analysis of the stress/strain (force/deformation) relationship governing the material response to an external perturbation, but at micron length scales [28]. This relationship is strongly dependent on the material structure and topology [29], thus micro-rheology techniques represent ideal candidates for the aim of this study. The linear stress/strain relationship of viscoelastic materials can be represented by the frequency-dependent dynamic complex modulus $G^*(\omega) = G'(\omega) + \mathrm{i}G''(\omega)$, which is defined as the ratio between the Fourier transforms (denoted by the symbol '$\wedge$') of the stress ($\sigma(t)$) and the strain ($\gamma(t)$),

$$G^*(\omega) = \frac{\hat{\sigma}(\omega)}{\hat{\gamma}(\omega)}. \quad (1)$$

The real and the imaginary components of $G^*(\omega)$ are also denoted as the storage, $G'(\omega)$, and the loss, $G''(\omega)$, moduli [30]; they provide information on both the elastic and the viscous nature of the material, respectively.

We present the first application of optical trapping to measure local variations in the micro-rheological properties of dissected vitreous humor. In this proof of principle study we observe regions showing varying degrees of viscoelasticity, along with the homogeneous and inhomogeneous nature of different regions of the vitreous humor.

2. Methods

2.1. Isolation of the rabbit vitreous humor

Vitreous samples were obtained from five New Zealand white rabbits, age range 33–64 weeks, weighing 2.3–4.0 kg respectively. The rabbits were euthanized and the eyes used secondary to another research project to minimize animal usage. The ophthalmic globe was dissected from the rabbit within 5 min of death. The globe was then washed with phosphate buffered saline (Sigma-Aldrich, Germany) to remove traces of blood. Subsequently, a 25-gauge needle was fitted to a 5 ml syringe and used to aspirate the aqueous humor to prevent contamination. An incision was made approximately 5 mm posterior to the limbus using a scalpel. Surgical scissors were used to cut along the sclera, taking care to separate the anterior from the posterior segment of the eye. On removal of the anterior segment, the adhesion between the lens and the anterior cortical vitreous gel was trimmed with a scalpel. The dissected vitreous was poured into an aluminum well with a conventional microscope coverslip superglued to the underside. Dry silica beads, 5 μm in diameter, were injected into the vitreous using a needle tip and were used as local probes. Figure 1 shows a schematic representation of the sample preparation process.

2.2. Optical trapping

A commercial inverted microscope (Nikon, TE2000U) formed the basis of the optical trapping system. A 532 nm continuous wave laser beam with a maximum power of 500 mW was provided by a frequency doubled Nd:YAG source (LASER2000, UK) and used to optically trap the beads, 532 nm being the maximum transmission wavelength for rabbit vitreous minimizing possible heating effects. The beam was elevated to the required height and expanded to fill the back aperture of the microscope objective (Nikon 100×, 1.3 NA Oil). Once a bead had been successfully trapped, the power of the laser beam was reduced to the minimum level at which the bead remained trapped using a variable neutral density filter. A camera (Proscilica, EC1280) was mounted on the side-port of the microscope and was capable of imaging at typically 300 frames s^{-1} when the region of interest was reduced to roughly 10 μm × 10 μm. The Brownian motion of the optically trapped bead was monitored using a modified version of the center-of-mass particle tracking software (LabVIEW, National Instruments) available from The University of Glasgow Optics Group website [31, 32]. Reference [32] provides details of the experimental error and minimum measurement achievable using this approach. A removable orange filter was placed in the illumination path just before the camera allowing the user to block the optical trapping laser beam when required. Figure 2 shows a schematic of the optical configuration [33].

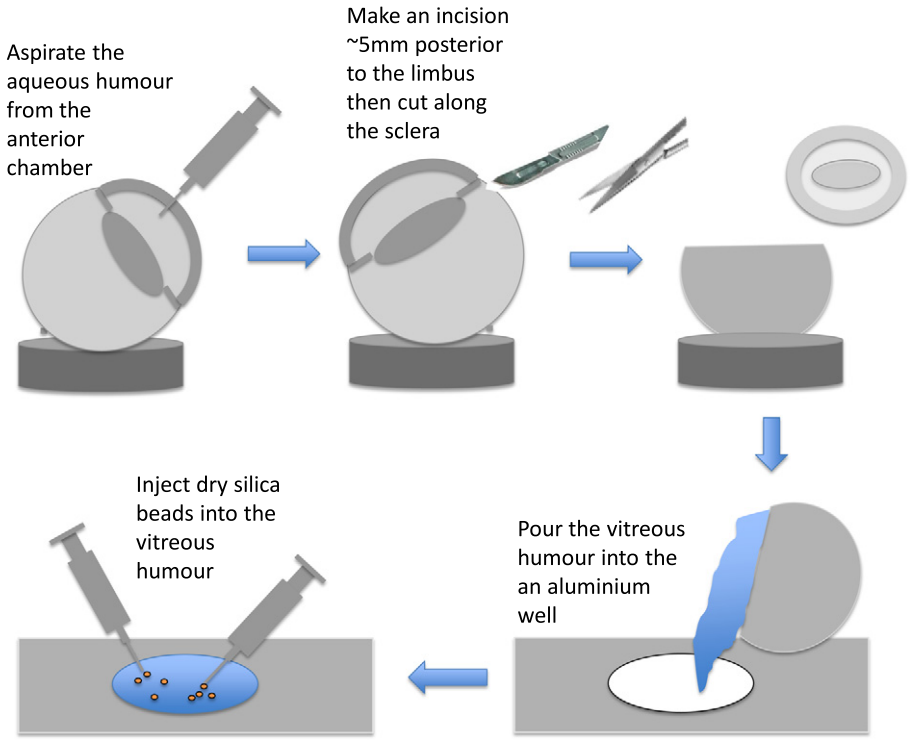

Figure 1. A schematic description of the sample preparation for micro-rheology measurements.

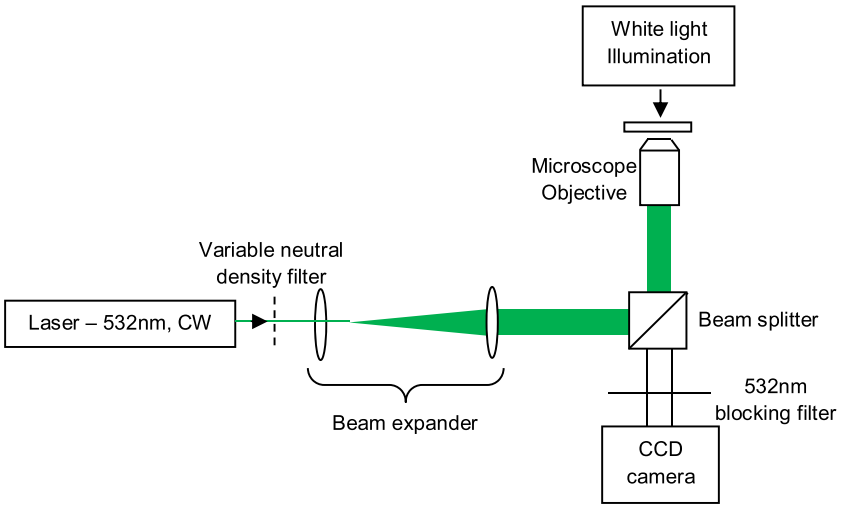

Figure 2. A schematic diagram of the optical tweezers setup.

2.3. Analytical model

The dynamics of an optically trapped bead are similar to those of a damped harmonic oscillator, where the restoring force is generated by the highly focused laser beam, the damping force is provided by the surrounding medium and the driving force is generated by the thermal energy of the system [18]. For small bead displacements (i.e. $\ll 0.8a$, where a is the bead radius), an optical trap can be modeled as a harmonic potential $E = \frac{1}{2}\kappa(r - r_0)^2$, where κ is the trap stiffness, r the bead position and r_0 the center of the optical trap (which is set equal to zero for simplicity, $r_0 = 0$). The trap stiffness can be calibrated using the principle of equipartition of energy (i.e. equating the potential energy to the thermal energy),

$$\tfrac{3}{2}k_{\mathrm{B}}T = \tfrac{1}{2}\kappa\langle r^2\rangle \qquad (2)$$

where k_{B} is the Boltzmann constant, T the absolute temperature and $\langle r^2\rangle$ the time-independent variance of the particle position r from the trap center (r_0). Importantly, this approach for calculating the trap stiffness is independent of both the viscoelasticity of the fluid under study and the particle size.

In order to resolve the viscoelastic properties of the vitreous humor using optical tweezers, we have adopted the analytical model developed by Tassieri *et al* [27] for a static

optical trap. They showed how the viscoelastic properties of a complex fluid can be revealed from analysis of the thermal fluctuation of an optically trapped bead, by means of its time-dependent mean-square displacement (MSD) defined as:

$$\langle \Delta r^2(\tau) \rangle = \langle [r(t+\tau) - r(t)]^2 \rangle_t \tag{3}$$

where t is the absolute time and τ the lag time (i.e. time interval since the start of the measurement). The average is taken over all initial times, t.

In particular, the relationship between the viscoelastic properties of the vitreous and the MSD of the bead is obtained by solving a generalized Langevin equation describing the three-dimensional bead position $\forall t$,

$$m\boldsymbol{a}(t) = \boldsymbol{f}_R(t) - \int_0^t \zeta(t-\tau)\boldsymbol{v}(\tau)\,\mathrm{d}\tau - \kappa \boldsymbol{r}(t) \tag{4}$$

where m is the mass of the bead, $\boldsymbol{a}(t)$ its acceleration, $\boldsymbol{v}(t)$ is the bead velocity, $-\kappa \boldsymbol{r}(t)$ is the trapping force and $\boldsymbol{f}_R(t)$ is the Gaussian white noise term, modeling the stochastic thermal forces acting on the particle. $\zeta(t)$ is a generalized memory function representing the viscoelastic nature of the fluid; i.e. the term of interest for micro-rheology studies. Following Mason and Weitz [34], the memory function can be related to the material's complex modulus via its Fourier transform, $\hat{\zeta}(\omega) = 6\pi a G^*(\omega)/\mathrm{i}\omega$. Therefore, equation (3) can be solved in terms of the complex modulus and the bead mean-square displacement:

$$G^*(\omega) = \frac{\kappa}{6\pi a}\left[\frac{1}{\mathrm{i}\omega\hat{\Pi}(\omega)} - 1\right] \tag{5}$$

where the inertia contribution $(m\omega^2)$ has been neglected and $\hat{\Pi}(\omega)$ is the Fourier transform of the normalized mean-squared displacement $\Pi(\tau) = \langle \Delta r^2(\tau) \rangle / 2\langle r^2 \rangle$. Note that $\Pi(\tau)$ is a dimensionless parameter and for a confined particle is equal to 1 at long time intervals (i.e. low frequencies).

3. Results

Prior to any set of measurements, a 5 μm bead was trapped in water to validate and calibrate the system. Figure 3 shows a log–log plot of the normalized mean-square displacement (NMSD, $\Pi(\tau)$) against lag time. The straight line represents the Einstein prediction for a freely diffusing bead in water.

From figure 3 it is clear that at short time intervals (thus small displacements) the bead behaves almost as if it were free to diffuse and the NMSD is in good agreement with the Einstein prediction. Whereas, at longer time intervals (thus large displacements), the bead is confined by the optical trap and the MSD plateaus to a maximum value equal to twice the variance, i.e. $\Pi(\tau)|_{\tau\to\infty} = 1$. Moreover, it is clear that the x and y components of the bead's motion overlap; revealing the same fluid dynamic properties. This is in agreement with what is expected for a laser beam with uniform illumination acting on a spherical particle suspended in an isotropic and homogeneous sample, water in this case.

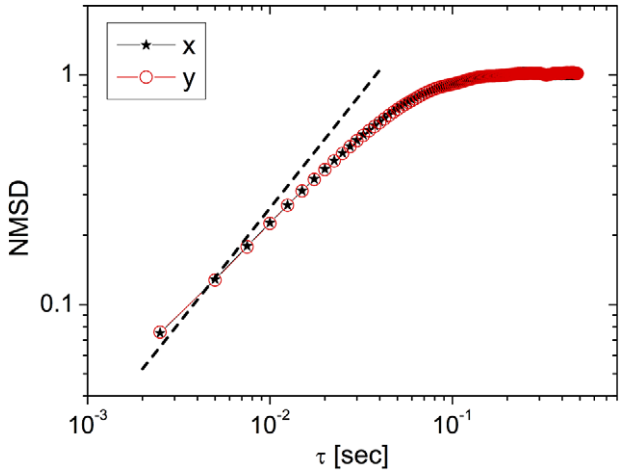

Figure 3. The normalized mean-square displacement (NMSD) plotted against lag time for a 5 μm diameter bead optically trapped in water. The dashed line represents the Einstein prediction for a freely diffusing bead in water, the overlay represents the X and Y components illustrating the uniformity of the trap.

Figures 4(A) and (B) show example plots of the NMSD and the relative complex moduli of beads trapped at different positions within the vitreous humor. In figure 4(A) at short time intervals the NMSD is almost linear (in a log–log plot) with a gradient significantly smaller than 1, indicating that the vitreous surrounding the trapped bead is behaving as a non-Newtonian fluid; whereas, at long time intervals the plateau region of the NMSD indicates the dominant effect of the optical trap. In figure 4(B), at short time scales (i.e. high frequencies), the NMSD is very close to 1; resembling the behavior of a weak gel, where the bead is predominantly confined by the gel network forming the vitreous rather than the optical trap. The viscoelastic moduli shown in figure 4 have been evaluated by analysis of the x component of the bead motion.

A local measure of the degree of inhomogeneity in the vitreous is provided by comparing the x and y components of the bead displacement. Figure 4(A) show an example of the local inhomogeneous nature of the vitreous humor where the motion of the optically trapped bead is different in x and y. It is important to highlight that a non-uniform laser beam profile could also lead to differences in the x and y displacements of the optically trapped bead. When a high numerical aperture objective lens is used to focus linearly polarized light it is common for an asymmetrical beam profile to occur. However, as shown in figure 3, for the case of a bead trapped in water (a homogeneous fluid) the two motion components clearly overlap; therefore, we can assume that our beam profile was uniform and not responsible for the effect reported in figure 4(A). The inhomogeneous nature of the vitreous humor is likely to be associated with the presence of the collagen fibers. Rabbit gel vitreous has a very dense collagen network compared to human [36]. The bead represented in figure 4(A) could well be trapped next to a collagen fiber (or bundle of fibers) that is hampering its movement in one axes as opposed to the other.

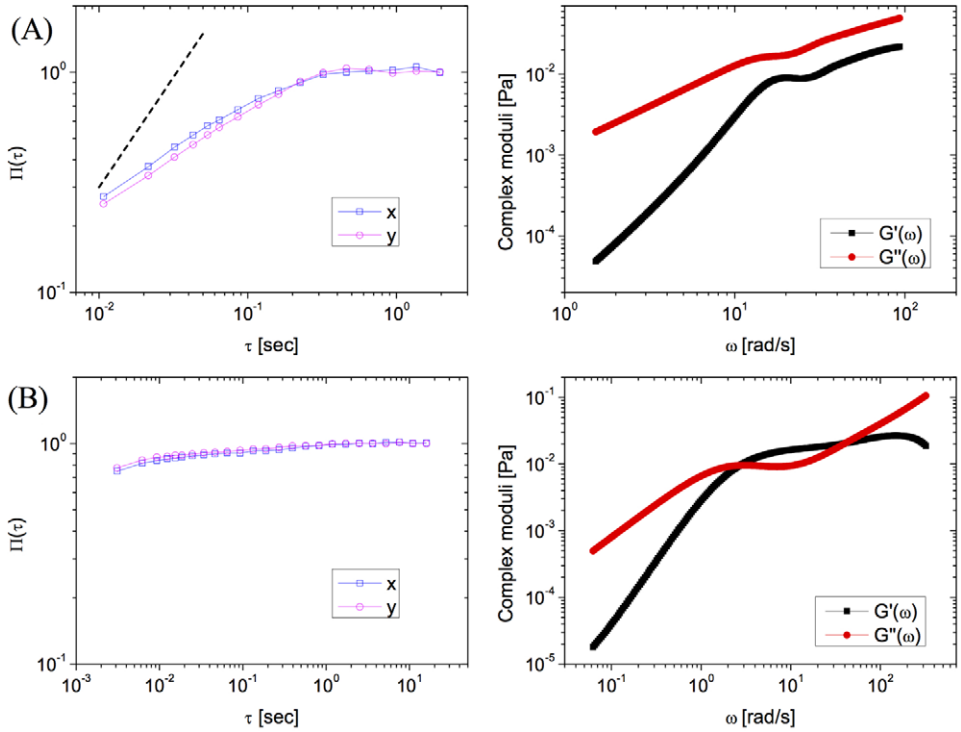

Figure 4. Example plots of the normalized mean-square displacement versus lag time for a 5 μm diameter bead optically trapped in vitreous humor, together with the relative complex moduli, $G'(\omega)$ and $G''(\omega)$, evaluated by means of equation (5) using the x component of the bead's motion. (A) shows a region of the vitreous that is behaving as a generic viscoelastic fluid, (B) a region where the vitreous is behaving as a complex fluid with a strong elastic character at high frequencies.

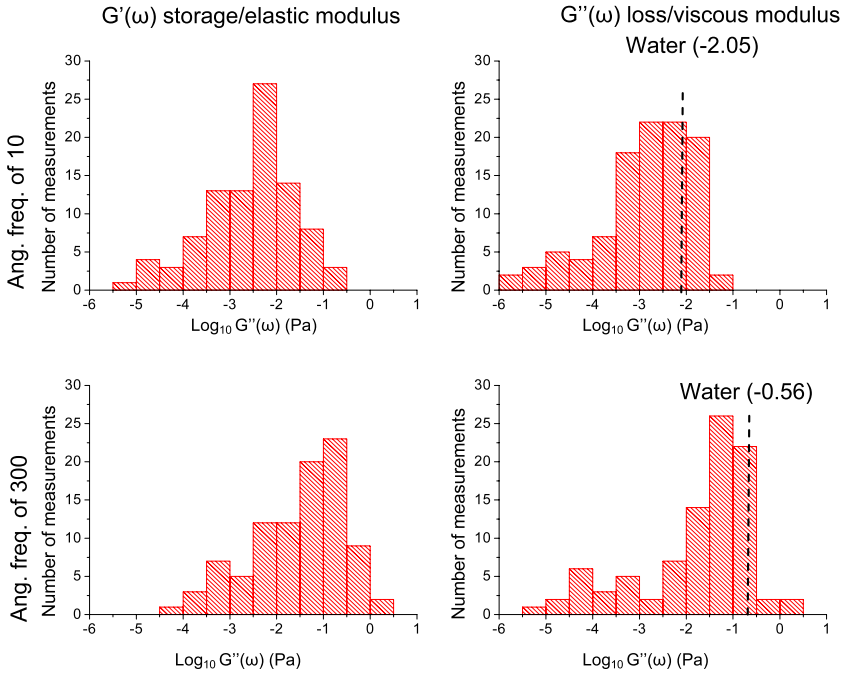

Figure 5. Combined results for 96 beads trapped in ten different vitreous samples. The histograms show Log_{10} of the loss and storage moduli at high (300 rad s^{-1}, bottom) and low (10 rad s^{-1}, top) angular frequencies. The dotted lines on the loss modulus plots represent the relative value for water for comparison.

As a further example of the vitreous humor inhomogeneity, Figure 5 presents data obtained from the analysis of 96 beads trapped in ten different samples of dissected vitreous humor. In particular, we report the Log_{10} of the loss and storage moduli measured at low (i.e. 10 rad s^{-1}) and high (i.e. 300 rad s^{-1}) angular frequencies. Figure 5 confirms that

the vitreous humor is far from uniform and, in each plot, G' or G'' can be seen to range over at least five orders of magnitude. The mean reading and standard deviation for the storage (elastic) modulus was 0.014 ±0.026 Pa at 10 rad s^{-1} and 0.14 ±0.26 Pa at 300 rad s^{-1}; whereas, for the loss (viscous) modulus the mean was 0.006±0.009 Pa at 10 rad s^{-1} and 0.11±0.23 Pa at 300 rad s^{-1}. The errors quoted relate to the standard deviation of the measurements and demonstrate the variability of the vitreous humor. Moreover, since 99% of the vitreous humor is water it is useful to compare the results presented in figure 5 to those of water at the same frequencies, see dotted lines on the loss modulus plots. In particular, at an angular frequency of 10 rad s^{-1} the mean value of the loss modulus for the vitreous is 0.006±0.009 Pa, which is very close to that of water of 0.0089 Pa; similar agreement is found at a higher angular frequency of 300 rad s^{-1} where the mean loss modulus of the vitreous is 0.11 ±0.23 Pa and that of water is 0.28 Pa. It can be seen in figure 5 that there is a low viscosity tail on both the loss modulus' histograms, where the measured viscosity sits below that of water; at present, the reasons for this are unknown. The loss modulus of water is measured using an optical trapping approach in [25] figure 5, and it is the values presented here that we have used for comparison.

4. Discussion

We have demonstrated that optical tweezers provide a suitable method for probing the micro-rheology (local rheology) of the vitreous humor. By optically trapping 5 μm diameter beads that had been injected into samples of dissected vitreous humor we were able to observe local changes in the micro-rheology of the vitreous, observations that would not be possible with conventional bulk rheometers. Regional variations in the rheological properties of the vitreous have also been reported by Lee and colleagues [7, 8] in human, cow and pig. Our data suggest that at high frequencies the rabbit vitreous shows a strong elastic behavior (similar to viscoelastic gels); this is in keeping with the findings reported by Mensitieri *et al* [35]. In view of the current research in investigating an effective intravitreal treatment, we believe that accurate information about the local viscoelastic properties of the vitreous humor will be useful during the design process of an optimum controlled-released drug delivery system.

In the future we aim to probe the properties of an aging eye where the contraction of vitreous protein elements leading to posterior retinal detachment creates an inhomogeneous compartment with the remnants of the vitreous sac floating in the liquid vitreous phase. The movement of drugs with low diffusion coefficients through this region of low viscosity will be affected to a greater extent by convective forces, which can influence drug exposure of the retinal tissues [37]. For this reason, vitreous rheology is an extremely relevant measurement in modeling the kinetics of drug movement in the posterior globe. Future approaches will allow the data to be correlated directly with specific regions within the intact vitreous either by improvements in the sample preparation/dissection techniques or by optically trapping beads injected into an intact perfused eye. The Miyake-Apple eye preparation technique, where a hole is made in the sclera of a dissected but intact eye and sealed using a microscope coverslip providing an optically transparent 'window' into the vitreous, shows a promising approach for achieving this.

5. Conclusion

We have demonstrated that an optically trapped bead can be used as a local probe to determine the micro-rheological properties of the vitreous humor. The vitreous humor was dissected from the ocular globe and 5 μm diameter dry silica beads injected into the sample to use as local probes. Using a fast camera and a center-of-mass particle tracking algorithm we monitored the displacement of the optically trapped bead with time. Analysis of the different frequency components of bead's motion provided local information about the medium surrounding the particle and allowed us to identify areas of the dissected vitreous that behaved as a complex viscoelastic fluid. In addition to this, we observed the homogeneous and inhomogeneous nature of the vitreous humor by comparing the motion of the bead in the x and y directions. It would not be possible to observe these features with the standard rheometers that give an average reading for the vitreous as a whole. The motivation behind this project is to aid the development of effective drug delivery techniques to treat retinal diseases such as age-related macular degeneration.

Acknowledgments

The authors are grateful to Professor Godfrey L Smith (University of Glasgow) for providing the rabbit eyes. LET acknowledges financial support from Allergan Inc. AJW and MT acknowledge support via personal research fellowships from the Royal Academy of Engineering/EPSRC.

References

[1] Bishop P 2000 *Prog. Retinal Eye Res.* **19** 323–44
[2] Sebag J 1998 *Prog. Polym. Sci.* **23** 415–46
[3] Sebag J 1989 *The Vitreous: Structure, Function and Pathobiology* (New York: Springer) pp 17–33
[4] Soman N and Banerjee R 2003 *Bio-med. Mater. Eng.* **13** 59–74
[5] Ciferri A and Magnasco A 2007 *Liq. Cryst.* **34** 219–27
[6] Bettelheim F A and Zigler J S 2004 *Exp. Eye Res.* **79** 713–8
[7] Lee B, Litt M and Buchsbaum G 1992 *Biorheology* **29** 521–33
[8] Lee B, Litt M and Buchsbaum G 1994 *Biorheology* **31** 327–38
[9] Lee B, Litt M and Buchsbaum G 1994 *Biorheology* **31** 339–51
[10] Jongebloed W L and Worst J F G 1987 *Documental Ophthalmol.* **67** 183–96
[11] Sebag J 2005 *Trans. Am. Ophthalmol. Soc.* **103** 473–94
[12] Sebag J 1987 *Graefe's Arch. Clin. Exp. Ophthalmol.* **225** 89–93
[13] Maurice D 2001 *J. Ocular Pharmacol. Therapeut.* **17** 393–401
[14] Tan L E, Orilla W, Hughes P M, Tsai S, Burke J A and Wilson C G 2011 *Invest. Ophthalmol. Vis. Sci.* **52** 1111–8
[15] Park J, Bungay P M, Lutz R J, Augsburger J J, Millard R W, Roy A S and Banerjee R K 2005 *J. Controll. Release* **105** 279–95
[16] Ashkin A, Dziedzic J M, Bjorkholm J E and Chu S 1986 *Opt. Lett.* **11** 228–90

[17] Molloy J E and Padgett M J 2002 *Contemp. Phys.* **43** 241–58
[18] Svoboda K and Block S M 1994 *Annu. Rev. Biophys. Biomol. Struct.* **23** 247–85
[19] Bishop A I, Nieminen T A, Heckenberg N R and Rubinsztein-Dunlop H 2004 *Phys. Rev. Lett.* **92** 198104
[20] Brau R R, Ferrer J M, Lee H, Castro C E, Tam B K, Tarsa P B, Matsudaira P, Boyce M C, Kamm R D and Lang M J 2007 *J. Opt. A: Pure Appl. Opt.* **9** S103–12
[21] Fischer M and Berg-Sørenson K 2007 *J. Opt.* A **9** S239–50
[22] Ługowski R, Kołodziejczyk B and Kawata Y 2002 *Opt. Commun.* **202** 1–8
[23] Pesce G, Sasso A and Fusco S 2005 *Rev. Sci. Instrum.* **76** 115105
[24] Pralle A, Florin E-L, Stelzer E H K and Hörber J K H 1998 *Appl. Phys.* A **66** S71–3
[25] Preece D, Warren R, Evans R M L, Gibson G M, Padgett M J, Cooper J M and Tassieri M 2011 *J. Opt.* **13** 044022
[26] Tassieri M, Gibson G M, Evans R M L, Yao A M, Warren R, Padgett M J and Cooper J M 2010 *Phys. Rev.* E **81** 026308
[27] Tassieri M, Evans R M L, Warren R L, Bailey N J and Cooper J M 2012 *New J. Phys.* **14** 115032
[28] Waigh T A 2005 *Rep. Prog. Phys.* **68** 685
[29] Liu J, Gardel M L, Kroy K, Frey E, Hoffman B D, Crocker J C, Bausch A R and Weitz D A 2006 *Phys. Rev. Lett.* **96** 118104
[30] Ferry J D 1980 *Viscoelastic Properties of Polymers* 3rd edn (New York: Wiley)
[31] www.physics.gla.ac.uk/Optics/projects/tweezers/software/
[32] Gibson G M, Leach J, Keen S, Wright A J and Padgett M J 2008 *Opt. Express* **16** 14561–70
[33] Watts F, Tan L-E, Tassieri M, McAlinden N, Wilson C G, Girkin J M and Wright A J 2011 *Proc. SPIE* **8097** 80970H
[34] Mason T G and Weitz D A 1995 *Phys. Rev. Lett.* **74** 1250–3
[35] Evans R M L 2009 *Br. Soc. Rheol. Bull.* **50** 76–86
[36] Mensitieri M, Ambrosio L, Nicolais L, Balzano L and Lepore D 1994 *J. Mater. Sci.: Mater. Med.* **5** 743–7
[37] Khathawate J and Acharya S 2008 *Int. J. Heat Mass Transfer* **51** 23–4